Investigation of the T-cells effect to the prediction of the atherosclerotic plaque development in carotid arteries

Dimitrios S. Pleouras, Michalis D. Mantzaris, Panagiotis K. Siogkas, Vassiliki T. Potsika, Vasilis D. Tsakanikas, Fragiska Sigala, and Dimitrios I. Fotiadis, *Fellow, IEEE*

***Abstract*— The carotid artery disease is one of the leading causes of mortality worldwide, as it leads to the progressive arterial stenosis that may result to stroke. To address this issue, the scientific community is attempting not only to enrich our knowledge on the underlying atherosclerotic mechanisms, but also to enable the prediction of the atherosclerotic progression. To this aim, this study investigates the role of T-cells in the atherosclerotic plaque growth process through the implementation of a computational model in realistic carotid arteries. In brief, T-cells mediate in the inflammatory process by secreting interferon-γ that enhances the activation of macrophages. In this analysis, we used 5 realistic human carotid arterial segments as input to the model. In particular, magnetic resonance imaging data, as well as, clinical data were collected from the patients at two time points. Using the baseline data, plaque growth was predicted and correlated to the follow-up arterial geometries. The results exhibited a very good agreement between them, presenting a high coefficient of determination, and thus of 0.64.**

***Clinical Relevance*— The presented methodology enables the prediction of the inflammatory response during the atherosclerotic process, that can be used as an additional tool for patient-specific risk stratification.**

I. Introduction

As recently as January 2021, COVID-19 was identified as the leading cause of death in USA, however, the carotid artery disease still remains a chronic and prevalent cause of mortality [1]. Atherosclerosis is the major cause of the carotid artery disease, which is identified by the presence of plaques within the carotid arteries, narrowing and stiffening them, and causing the reduction of the brain's blood supply, that may lead to strokes or transient ischemic attacks (TIA). According to histological analyses, the atherosclerotic plaques consist of cholesterol, calcium, fibrous tissue and other cellular debris, while they differentiate into 8 types according to the American Heart Association (AHA) [2]. Specifically, the underlying biological process of the atherosclerotic plaque generation is very complicated; however, over the past century, the major risk factors have been discovered, identifying high serum lipids, smoking, diabetes and obesity as the major culprits of atherosclerosis [3].

Currently, prevention of atherosclerosis is based on the regulation of the patient's diet and exercise program, or in provision of medications to lower the serum lipids. However, in case of an ischemic event, several procedures are available, including medication or/and surgery. The main treatment is the provision of intravenous tissue plasminogen activator (tPA), which breaks up clots, while medication is provided to restore breathing, heart rate and blood pressure. In case tPA has no effect, clots can be removed through surgery up to 24 hours after the onset of stroke symptoms [4].

However, an era of change in the prevention and treatment of the carotid artery disease is forced by the advance in the technological and biological field. The first pieces of evidence include the constant enrichment of our knowledge regarding the atherosclerotic mechanisms, and the initiation of the attempts to predict the atherosclerotic plaque growth using computational techniques. Regarding the last one, the most common approaches are based on the accumulation of lipoproteins within the arterial wall that trigger several pathophysiological pathways resulting to atherosclerosis [5].

Briefly, one of the most representative models considers that the atherosclerotic process initiates with the effect of the shear stress on the endothelial membrane due to blood flow [6]. This triggers a specific pathway that may result to endothelial dysfunction causing an increased endothelial permeability, thus favoring the abnormal accumulation of low-density lipoproteins (LDL) within the arterial wall. Within the arterial wall, LDL is oxidized triggering an inflammatory response by the production of cytokines, which are inflammatory mediators. The inflammatory response includes the accumulation of monocytes and their differentiation into macrophages, that uptake the oxidized LDL and form foam cells and consequently fatty streaks. In addition, the contractile smooth muscle cells (SMCs) proliferate and differentiate into synthetic SMCs secreting collagen to restore the area of inflammation. Overall, this results in the generation of plaque, increasing the wall thickness, while reducing the lumen area [7].

Several attempts have been made to accurately predict atherosclerotic plaque growth, implementing one or more of the abovementioned mechanisms. However, most of these studies utilized idealized 1D or 2D arterial geometries [8],

* This work has received funding from the European Union's Horizon 2020 research and innovation programme under grant agreement No 755320, as part of the TAXINOMISIS project.

D. S. Pleouras, M. D. Mantzaris, P. K. Siogkas, V. D. Tsakanikas, and V. T. Potsika are with the Unit of Medical Technology and Intelligent Information Systems, Department of Materials Science and Engineering University of Ioannina, Ioannina, Greece (e-mail: dipleouras@gmail.com, dmantzaris@gmail.com, siogkas4454@gmail.com, vasilistsakanikas@gmail.com, potsika@gmail.com).

F. Sigala is with the First Propaedeutic Department of Surgery, National and Kapodistrian University of Athens, Hippocration Hospital, Athens, Greece.

D. I. Fotiadis is with the Unit of Medical Technology and Intelligent Information Systems, Department of Materials Science and Engineering, University of Ioannina, and with the Department of Biomedical Research, Institute of Molecular Biology and Biotechnology–FORTH, University Campus of Ioannina, 45110 Ioannina, Greece (phone: +30 26510 09006; email: fotiadis@uoi.gr).

while only a few proof-of-concept studies are based on realistic human arterial geometries [7], [9]–[14].

In this case-study, we developed a novel model for the prediction of atherosclerotic plaque growth including the effect of the T-cells in the atherosclerotic process, which was implemented in realistic human 3D reconstructed carotid arterial segments. T-cells have been implicated in mediating many aspects of autoimmune inflammation. Specifically, T-cells accumulate within the arterial wall and activate in contact with the macrophage-secreted interleukin-12 (IL-12), which is an inflammatory mediator. The activated T-cells secrete interferon-γ (IFN-γ) that enhances the activity of macrophages and thus, contributing to the generation of plaques [15].

II. Materials & Methods

A. Dataset

The presented model was employed to a dataset of 5 human carotid arteries for its validation. This dataset includes the magnetic resonance imaging (MRI) data of the carotid arterial segments at two time points with interscan interval of 1 year, as well as the corresponding clinical data of each patient. Each patient provided written informed consent and enrolled in the TAXINOMISIS clinical study (www.clinicaltrials.gov; ID: NCT03495830) protocol which was approved by the local competent ethics committee.

B. 3D Reconstruction of carotid arteries and their plaque components

The 3D carotid arterial geometries are reconstructed based on a series of magnetic resonance imaging (MRI) modalities, including ToF, T1w, T2w and PD series. More specifically, TOF series are utilized to reconstruct the lumen of the 3D model while the fusion of T1w, T2w and PD series are utilized for the reconstruction of the arterial wall model, as well as the model of the plaque components. Finally, the three resulting models are aligned for constituting the final arterial model.

The creation of each of the aforementioned models is based on a novel methodology which comprises of three steps:

a) Segmentation of the region of interest: For segmenting the regions of interest (lumen, outer wall and plaque components), three deep learning models have been created. More specifically, two experts have annotated 485 tuples of ToF, T1w, T2w and PD images from 42 different patients. This process resulted in a training dataset which was used to train three UNET models for the aforementioned region of interest.

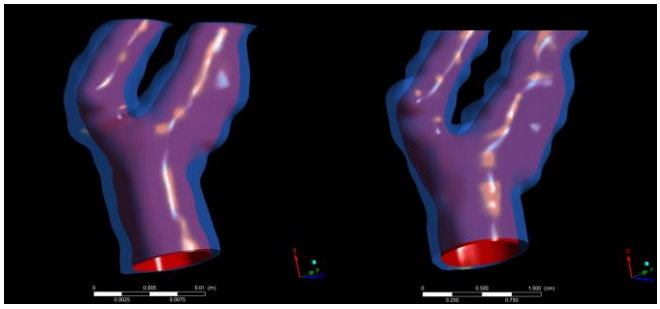

Fig 1. A case example of the baseline (left) and the follow-up (right) of a carotid arterial segment.

b) 3D level set: A morphological operator is applied to the 3D volume of the stacked 2D segmented frames in order to produce the 3D surface model.

c) 3D meshing: Marching cubes algorithm is applied to the 3D surface model, resulting to the final reconstructed arterial model.

A. Plaque Growth Model

In our approach, we incorporated the effect of T-cells in a previously validated plaque growth model, as presented in a proof-of-concept study [7]. This model is separated in three modeling levels: i) simulation of the blood flow, ii) simulations of the biological processes within the arterial wall and iii) simulation of wall thickening. The derived plaque components are calculated based on the concentrations of foam cells, collagen and smooth muscle cells.

a) T-cell infiltration through endothelium: We assume that T-cells infiltrate within the arterial wall in a steady rate (=0.05 cm^{-1} [15]), which is part of the inflammatory response. Therefore, the following flux boundary condition for T-cells (eq. 1) is applied to the endothelial membrane.

$$\frac{\partial c_T}{\partial \boldsymbol{n}} + a_T\left(c_T - c_{T_0}\right) = 0, \tag{1}$$

where, c_T is the concentration of the T-cells in the outer side of the endothelial membrane, and c_{T_0} (=10^{-3} gcm^{-3} [15]) is the average T-cell concentration in blood.

b) The T-cell activator, IL-12: Macrophages, foam cells and SMCs secrete interleukin-12 (IL-12), which activates T-cells in order to respond to the inflammatory process. IL-12 concentration is described by the following diffusion-reaction equation (eq. 2) [15].

$$\begin{aligned} &\gamma\frac{\partial c_{IL_{12}}}{\partial t} - D_{IL_{12}}\frac{\partial}{\partial x_i}\left(\boldsymbol{K}\cdot\frac{\partial}{\partial x_j}c_{IL_{12}}\right) \\ &= \gamma\lambda_{IL_{12}M}\frac{c_M}{K_M + c_M}\left(1 + \frac{c_{IFN-\gamma}}{K_{IL_{12}}c_{HDL} + c_{IFN-\gamma}}\right) \\ &\quad + \gamma\lambda_{IL_{12}F}\frac{c_F}{K_F + c_F} - \gamma d_{IL_{12}}c_{IL_{12}}, \end{aligned} \tag{2}$$

$$K^{ij} = \gamma\delta^{ij}, \tag{3}$$

where, $c_{IL_{12}}$, c_M, $c_{IFN-\gamma}$, c_{HDL}, c_F are the concentrations of IL-12, macrophages, INF-γ, HDL and foam cells respectively, γ (=0.96 [16]) is the porosity of the arterial wall, $\boldsymbol{K}$ is the area porosity tensor (which is a symmetric second rank tensor),, $D_{IL_{12}}$ (=1.08x10^2 cm^2day^{-1} [17]) is the diffusivity of IL-12, $\lambda_{IL_{12}M}$ (=3x10^{-7} $gcm^{-3}day^{-1}$ [18]) is the production rate of IL-12 by macrophages, $\lambda_{IL_{12}F}$ (=1x10^{-7} $gcm^{-3}day^{-1}$ [18]) is production rate of IL-12 by foam cells, $K_M = K_F$ have the half value of c_{M_0} (=5x10^{-3} gcm^{-3} [19]), which is the average concentration of macrophages in blood, $K_{IL_{12}}$ (=7x10^{-11} gcm^{-3} [18]) is the IFN-γ saturation for the production of IL-12, and $d_{IL_{12}}$ (=1.188 day^{-1} [20], [21]) is the degradation rate of IL-12.

c) T-cell dynamics: The concentration of T-cells (primarily CD4+ T-cells) is modeled by the following convection-diffusion-reaction equation (eq 4).

$$\gamma\frac{\partial c_T}{\partial t}+\frac{\partial}{\partial x_i}\left((\boldsymbol{K}\cdot\boldsymbol{U})_j c_T\right)-D_T\frac{\partial}{\partial x_i}\left(\boldsymbol{K}\cdot\frac{\partial}{\partial x_j}c_T\right)=\gamma\lambda_{TIL_{12}}\frac{c_M}{K_M+c_M}c_{IL_{12}}-\gamma d_T c_T, \quad (4)$$

where, D_T (=8.64x10^{-7} cm^{2}day^{-1} [22]) is the diffusivity of the T-cells, $\lambda_{TIL_{12}}$ (=1x10^6 day^{-1} [20], [21]) is the activation rate of the T-cells by IL-12, d_T (=0.33 day^{-1} [20], [21]) is the degradation rate of T-cells.

d) IFN-γ dynamics: The T-cell secreted IFN-γ is described by the following diffusion-reaction equation (eq. 5).

$$\gamma\frac{\partial c_{IFN-\gamma}}{\partial t}-D_{IFN-\gamma}\frac{\partial}{\partial x_i}\left(\boldsymbol{K}\cdot\frac{\partial}{\partial x_j}c_{IFN-\gamma}\right)=\gamma\lambda_{IFN-\gamma T}c_T-\gamma d_{IFN-\gamma}c_{IFN-\gamma}, \quad (5)$$

where, $D_{IFN-\gamma}$ (=1.08x10^2 cm^{2}day^{-1} [23]) is the diffusivity of the INF-γ, $\lambda_{IFN-\gamma T}$ (=0.066 day^{-1} [17]) is the production rate of IFN-γ by T-cells, and (=0.69 day^{-1} [24]) is the degradation rate of IFN-γ.

ε) Monocyte & Macrophage dynamics: The monocyte and macrophage concentrations are based on the following convection-diffusion-reaction equations (eq. 6 & eq.7), which have been altered in relation to the model presented in [7], in order to consider the effect of IFN-γ.

$$\gamma\frac{\partial c_{monocytes}}{\partial t}-D_{monocytes}\frac{\partial}{\partial x_i}\left(\boldsymbol{K}\cdot\frac{\partial}{\partial x_j}c_{monocytes}\right)-\gamma\lambda_{MIFN-\gamma}\frac{c_{IFN-\gamma}}{K_{IFN-\gamma}+c_{IFN-\gamma}}c_{monocytes}=-\gamma m_d c_{monocytes}, \quad (6)$$

$$\gamma\frac{\partial c_{Macrophages}}{\partial t}-D_{Macrophages}\frac{\partial}{\partial x_i}\left(\boldsymbol{K}\cdot\frac{\partial}{\partial x_j}c_{Macrophages}\right)=\gamma\lambda_{MIFN-\gamma}\frac{c_{IFN-\gamma}}{K_{IFN-\gamma}+c_{IFN-\gamma}}c_{monocytes}-\gamma k_1 c_{Macrophages}, \quad (7)$$

where, $c_{monocytes}$, $c_{Macrophages}$, $D_{monocytes}$ and $D_{Macrophages}$ are the concentrations and the diffusivities of monocytes and macrophages respectively, $\lambda_{MIFN-\gamma}$ (=0.005 day^{-1} [20]) is the activation rates of macrophages by IFN-γ, m_d (= 2.572 s^{-1} [25]) is the apoptosis rate of monocytes, $K_{IFN-\gamma}$ (=1x10^{-11} gcm^{-3} [20]), and k_1 (=0.0367x10^{-4} m^{3}cells^{-1}s^{-1} [26]) is the macrophage differentiation rate into foam cells.

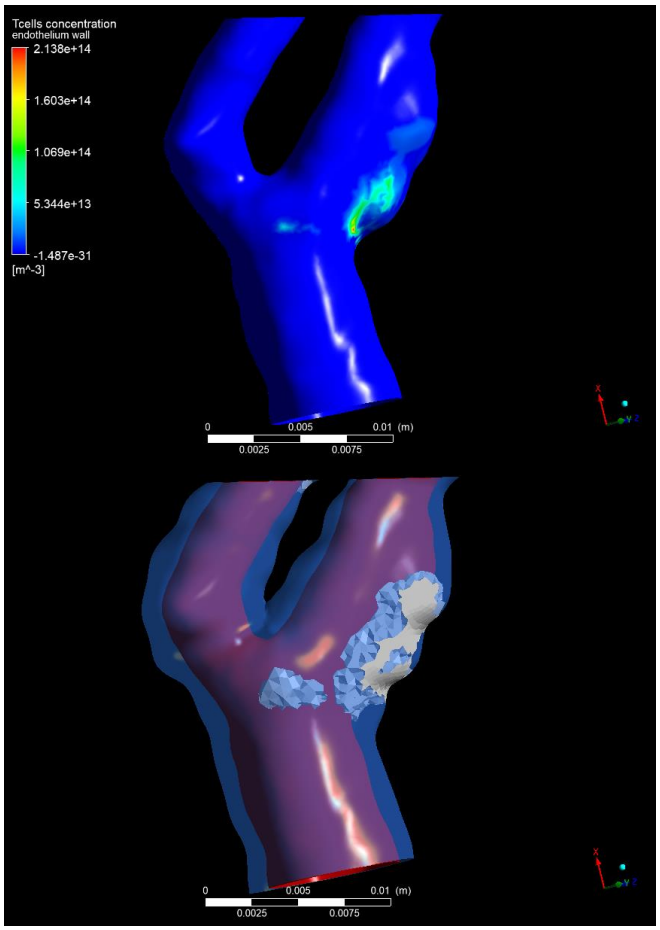

Fig. 2. A case example of the T-cell concentration distribution and plaque formation of a carotid arterial segment.

III. Results

We reconstructed 5 carotid arteries at the two time-points, using the available MRI data. The plaque growth model was implemented to the baseline geometries, and resulted to the wall-thickened geometries, along with several plaque regions (fig. 2). The results indicated that the multi-level computational model can be used for the prediction of regions which are prone to plaque progression. Specifically, we tested the validity of our approach by comparing the predicted geometries to the corresponding follow-up using a well-accepted measure of comparison as a benchmark, which is the comparison of the area values of common cross-sections [7], [9]. In accordance to this benchmark, we performed the manual registration of the baseline and follow-up geometries, and then, the cross-sections were extracted with an intermediate spacing of 0.5mm. To avoid any registration error of the previous procedure, the comparison was performed utilizing the mean areas of every six cross-sections as a benchmark.

The results indicated that the main volume of the predicted plaque and the corresponding lumen stenosis coincided with the realistic follow-up stenosis. Moreover, in order to extract a quantitative correlation of the results, we performed a regression analysis between the real follow-up and the simulated geometries. The correlation between the simulated and the follow-up cross-section areas, resulted to a coefficient of determination R^2=0.64.

IV. Conclusion

In this study, it was assumed that T-cells infiltrate within the arterial wall with a steady flux rate regardless of the arterial region. Although, the attraction and infiltration of T-cells within the arterial wall is far more complicated, their effect to the activation of macrophages is described sufficiently, so that the results demonstrated that the presented plaque growth model can predict the plaque progression in comparison with the realistic follow-up plaques.

To our knowledge, this is the first study that evaluates the arterial wall thickening, as well as, the lumen stenosis in 3D reconstructed carotid arterial segments using a plaque growth model that considers the effect of T-cells to the inflammatory process.

References

[1] "Home." https://www.who.int (accessed Jan. 14, 2022).

[2] J.-M. Cai, T. S. Hatsukami, M. S. Ferguson, R. Small, N. L. Polissar, and C. Yuan, "Classification of Human Carotid Atherosclerotic Lesions With In Vivo Multicontrast Magnetic Resonance Imaging," *Circulation*, vol. 106, no. 11, pp. 1368–1373, Sep. 2002, doi: 10.1161/01.CIR.0000028591.44554.F9.

[3] P. Libby, "History of Discovery: Inflammation in Atherosclerosis," p. 15, 2013.

[4] W. J. Powers *et al.*, "2018 Guidelines for the Early Management of Patients With Acute Ischemic Stroke: A Guideline for Healthcare Professionals From the American Heart Association/American Stroke Association," *Stroke*, vol. 49, no. 3, Mar. 2018, doi: 10.1161/STR.0000000000000158.

[5] H. C. Stary, "Natural History and Histological Classification of Atherosclerotic Lesions," *Arteriosclerosis, Thrombosis, and Vascular Biology*, vol. 20, no. 5, pp. 1177–1178, May 2000, doi: 10.1161/01.ATV.20.5.1177.

[6] A. I. Sakellarios *et al.*, "Modelling LDL accumulation in the case of endothelial dysfunction," vol. 5, no. 2, p. 11, 2011.

[7] D. S. Pleouras *et al.*, "Simulation of atherosclerotic plaque growth using computational biomechanics and patient-specific data," *Sci Rep*, vol. 10, no. 1, p. 17409, Dec. 2020, doi: 10.1038/s41598-020-74583-y.

[8] M. Guo, Y. Cai, X. Yao, and Z. Li, "Mathematical modeling of atherosclerotic plaque destabilization: Role of neovascularization and intraplaque hemorrhage," *Journal of Theoretical Biology*, vol. 450, pp. 53–65, Aug. 2018, doi: 10.1016/j.jtbi.2018.04.031.

[9] A. I. Sakellarios *et al.*, "Prediction of Atherosclerotic Plaque Development in an In Vivo Coronary Arterial Segment Based on a Multilevel Modeling Approach," *IEEE Trans. Biomed. Eng.*, vol. 64, no. 8, pp. 1721–1730, Aug. 2017, doi: 10.1109/TBME.2016.2619489.

[10] A. Sakellarios *et al.*, "Prediction of atherosclerotic disease progression using LDL transport modelling: a serial computed tomographic coronary angiographic study," *Eur Heart J Cardiovasc Imaging*, vol. 18, no. 1, pp. 11–18, Jan. 2017, doi: 10.1093/ehjci/jew035.

[11] D. Pleouras *et al.*, "Atherosclerotic Plaque Growth Prediction in Coronary Arteries using a Computational Multi-level Model: The Effect of Diabetes," in *2019 IEEE 19th International Conference on Bioinformatics and Bioengineering (BIBE)*, Athens, Greece, Oct. 2019, pp. 702–705. doi: 10.1109/BIBE.2019.00132.

[12] D. Pleouras *et al.*, "A computational multi-level atherosclerotic plaque growth model for coronary arteries," in *2019 41st Annual International Conference of the IEEE Engineering in Medicine and Biology Society (EMBC)*, Jul. 2019, pp. 5010–5013. doi: 10.1109/EMBC.2019.8857329.

[13] P. Siogkas *et al.*, "Multiscale - Patient-Specific Artery and Atherogenesis Models," *IEEE Trans. Biomed. Eng.*, vol. 58, no. 12, pp. 3464–3468, Dec. 2011, doi: 10.1109/TBME.2011.2164919.

[14] M. D. Mantzaris *et al.*, "Computational modeling of atherosclerotic plaque progression in carotid lesions with moderate degree of stenosis *," in *2021 43rd Annual International Conference of the IEEE Engineering in Medicine & Biology Society (EMBC)*, Mexico, Nov. 2021, pp. 4209–4212. doi: 10.1109/EMBC46164.2021.9630376.

[15] W. Hao and A. Friedman, "The LDL-HDL Profile Determines the Risk of Atherosclerosis: A Mathematical Model," *PLoS ONE*, vol. 9, no. 3, p. e90497, Mar. 2014, doi: 10.1371/journal.pone.0090497.

[16] L. Ai and K. Vafai, "A coupling model for macromolecule transport in a stenosed arterial wall," *International Journal of Heat and Mass Transfer*, vol. 49, no. 9–10, pp. 1568–1591, May 2006, doi:1016/j.ijheatmasstransfer.2005.10.041.

[17] K. Tsukaguchi, K. N. Balaji, and W. H. Boom, "CD4+ alpha beta T cell and gamma delta T cell responses to Mycobacterium tuberculosis. Similarities and differences in Ag recognition, cytotoxic effector function, and cytokine production," *J Immunol*, vol. 154, no. 4, pp. 1786–1796, Feb. 1995.

[18] J. Day, A. Friedman, and L. S. Schlesinger, "Modeling the immune rheostat of macrophages in the lung in response to infection," *Proc Natl Acad Sci U S A*, vol. 106, no. 27, pp. 11246–11251, Jul. 2009, doi: 10.1073/pnas.0904846106.

[19] M. Kroll, "Tietz Textbook of Clinical Chemistry," *Clinical Chemistry*, vol. 45, no. 6, pp. 913–914, Jun. 1999, doi: 10.1093/clinchem/45.6.913.

[20] A. Friedman, J. Turner, and B. Szomolay, "A model on the influence of age on immunity to infection with Mycobacterium tuberculosis," *Exp Gerontol*, vol. 43, no. 4, pp. 275–285, Apr. 2008, doi: 10.1016/j.exger.2007.12.004.

[21] I. M. Orme, "Aging and immunity to tuberculosis: increased susceptibility of old mice reflects a decreased capacity to generate mediator T lymphocytes," *J Immunol*, vol. 138, no. 12, pp. 4414–4418, Jun. 1987.

[22] Y. Kim, S. Roh, S. Lawler, and A. Friedman, "miR451 and AMPK Mutual Antagonism in Glioma Cell Migration and Proliferation: A Mathematical Model," *PLOS ONE*, vol. 6, no. 12, p. e28293, Dec. 2011, doi: 10.1371/journal.pone.0028293.

[23] K.-L. Liao, X.-F. Bai, and A. Friedman, "The role of CD200-CD200R in tumor immune evasion," *J Theor Biol*, vol. 328, pp. 65–76, Jul. 2013, doi: 10.1016/j.jtbi.2013.03.017.

[24] Y. Kim and A. Friedman, "Interaction of tumor with its micro-environment: A mathematical model," *Bull Math Biol*, vol. 72, no. 5, pp. 1029–1068, Jul. 2010, doi: 10.1007/s11538-009-9481-z.

[25] R. V. Krstić, *Human Microscopic Anatomy*. Berlin, Heidelberg: Springer Berlin Heidelberg, 1991. doi: 10.1007/978-3-662-02676-2.

[26] H. S. Kruth, W. Huang, I. Ishii, and W.-Y. Zhang, "Macrophage foam cell formation with native low density lipoprotein," *J Biol Chem*, vol. 277, no. 37, pp. 34573–34580, Sep. 2002, doi: 10.1074/jbc.M205059200.